Mechanism of IL-1β Modulation of Intestinal Epithelial Barrier Involves p38 Kinase and Activating Transcription Factor-2 Activation

Rana Al-Sadi,* Shuhong Guo,* Dongmei Ye,* Karol Dokladny,* Tarik Alhmoud,* Lisa Ereifej,* Hamid M. Said,[†,‡] and Thomas Y. Ma*[,§]

The defective intestinal epithelial tight junction (TJ) barrier has been postulated to be an important pathogenic factor contributing to intestinal inflammation. It has been shown that the proinflammatory cytokine IL-1β causes an increase in intestinal permeability; however, the signaling pathways and the molecular mechanisms involved remain unclear. The major purpose of this study was to investigate the role of the p38 kinase pathway and the molecular processes involved. In these studies, the in vitro intestinal epithelial model system (Caco-2 monolayers) was used to delineate the cellular and molecular mechanisms, and a complementary in vivo mouse model system (intestinal perfusion) was used to assess the in vivo relevance of the in vitro findings. Our data indicated that the IL-1β increase in Caco-2 TJ permeability correlated with an activation of p38 kinase. The activation of p38 kinase caused phosphorylation and activation of p38 kinase substrate, activating transcription factor (ATF)-2. The activated ATF-2 translocated to the nucleus where it attached to its binding motif on the myosin L chain kinase (MLCK) promoter region, leading to the activation of MLCK promoter activity and gene transcription. Small interfering RNA induced silencing of ATF-2, or mutation of the ATF-2 binding motif prevented the activation of MLCK promoter and MLCK mRNA transcription. Additionally, in vivo intestinal perfusion studies also indicated that the IL-1β increase in mouse intestinal permeability required p38 kinase–dependent activation of ATF-2. In conclusion, these studies show that the IL-1β–induced increase in intestinal TJ permeability in vitro and in vivo was regulated by p38 kinase activation of ATF-2 and by ATF-2 regulation of MLCK gene activity. *The Journal of Immunology*, **2013, 190: 6596–6606.**

The defective intestinal epithelial tight junction (TJ) barrier, leading to an increased intestinal penetration of luminal bacterial Ags, has been postulated to be an important pathogenic factor contributing to the development of intestinal inflammation (1–3). Patients with Crohn disease have an increase in intestinal permeability (2–4). A persistent increase in intestinal permeability following medical therapy was associated with poor clinical outcome in patients with Crohn disease, whereas normalization of intestinal permeability following medical therapy was predictive of a prolonged clinical remission (5, 6). Similarly, in IL-10–deficient mice (IL-$10^{-/-}$), a commonly used animal model of Crohn disease, the development of intestinal inflammation was preceded by an increase in intestinal permeability (7, 8). Additionally, pharmacologic enhancement of intestinal TJ barrier with AT-1001 (a zonulin peptide inhibitor) prevented the development of intestinal inflammation in IL-$10^{-/-}$ mice, suggesting that the defective intestinal TJ barrier was necessary for the development of intestinal inflammation (1). The importance of the luminal Ag in the development of intestinal inflammation has also been confirmed by studies showing that germ-free or antibiotic-treated mice do not develop intestinal inflammation (8).

IL-1β is a prototypical proinflammatory cytokine that plays a central role in the inflammatory responses of the gut (9, 10). Patients with Crohn disease have elevated levels of IL-1β in their intestinal tissue, and the level of IL-1β elevation correlates with the severity of intestinal inflammation (11–13). There is an imbalance of IL-1β and its naturally occurring antagonist IL-1ra in the intestinal tissue of patients with Crohn disease, suggesting a lack of intrinsic ability to counteract the proinflammatory effects of IL-1β (13, 14). Recent studies have also identified an existence of IL-1β gene polymorphism in Crohn disease patients that determines the severity of inflammation in the affected patients (15). In animal studies, exogenous administration of IL-1ra resulted in improvement of experimental colitis (16, 17). However, note that in small studies, the treatment of Crohn disease patients with IL-1ra analog (anakinra) did not appear to have significant therapeutic benefits (18, 19).

In addition to its direct immune-activating effects, IL-1β also causes an increase in intestinal TJ permeability (11, 20). The IL-1β–induced increase in intestinal TJ permeability has been postulated to be an important factor contributing to the development of intestinal inflammation by allowing increased intestinal permeation of luminal Ags (21, 22). Previous studies from our laboratory have suggested that the IL-1β–induced increase in intestinal TJ permeability was related to an activation of the myosin L chain kinase (MLCK) gene and an increase in gene transcription (23, 24). However, the intracellular signaling pathways and the

*Department of Internal Medicine, University of New Mexico School of Medicine, Albuquerque, NM 87131; [†]Department of Medicine, University of California, Irvine, Irvine, CA 92617; [‡]Department of Veterans Affairs Medical Center, Long Beach, CA 90822; and [§]Albuquerque Veterans Affairs Medical Center, Albuquerque, NM 87108

Received for publication July 6, 2012. Accepted for publication March 25, 2013.

This work was supported by a Veterans Affairs Merit Review grant from the Veterans Affairs Research Service and by National Institute of Diabetes and Digestive and Kidney Diseases Grants R01-DK-64165 and R01-DK-081429 (to T.Y.M.).

Address correspondence and reprint requests to Dr. Thomas Y. Ma, Internal Medicine-Gastroenterology, Mail Stop Code 10 5550, University of New Mexico, Albuquerque, NM 87131-0001. E-mail address: tma@salud.unm.edu

Abbreviations used in this article: ATF, activating transcription factor; IBD, inflammatory bowel disease; MDCK, Madin–Darby canine kidney; MLCK, myosin L chain kinase; RT, reverse transcription; siRNA, small interfering RNA; TER, transepithelial electrical resistance; TJ, tight junction.

transcriptional regulators that mediate IL-1β modulation of the MLCK gene and the intestinal barrier remain unclear.

The major aims of this study were to investigate the signaling pathways and the transcriptional regulators involved in the IL-1β modulation of intestinal epithelial TJ barrier. In this study, we used a complementary in vitro (filter-grown Caco-2 monolayers) and in vivo (live mouse intestinal perfusion) model systems to assess the intracellular and molecular mechanisms involved and to validate the in vivo relevance of the signaling and molecular studies. Because the p38 kinase signaling pathway has been implicated in many of the biological activities of IL-1β, we investigated the role of the p38 kinase pathway in the IL-1β effect. Our data suggested that the IL-1β–induced increase in intestinal TJ permeability was regulated in part by the activation of the p38 kinase signaling cascade and p38-kinase dependent activation of nuclear transcription factor activating transcription factor (ATF)-2.

Materials and Methods

Chemicals

Cell culture media (DMEM), trypsin, FBS, glutamine, penicillin, streptomycin, and PBS were purchased from Life Technologies BRL (Grand Island, NY). Anti–p38 kinase, phospho–p38 kinase, MLCK, and anti–β-actin Abs were obtained from Sigma-Aldrich (St. Louis, MO). Anti–ATF-2 and phospho–ATF-2 Abs were purchased from Abcam (Cambridge, MA). HRP-conjugated secondary Abs for Western blot analysis were purchased from Invitrogen (San Francisco, CA). Small interfering RNA (siRNA) of p38 kinase, ATF-2, Accell medium, and transfection reagents were obtained from Dharmacon (Lafayette, CO). SB-203580 and SB-202474 were purchased from Sigma-Aldrich (St. Louis, MO). All other chemicals were purchased from Sigma-Aldrich/VWR International (West Chester, PA) or Fisher Scientific (Pittsburgh, PA).

Cell cultures

Caco-2 cells (passage 20–26) were purchased from the American Type Culture Collection (Rockville, MD) and maintained at 37°C in a culture medium composed of DMEM with 4.5 mg/ml glucose, 50 U/ml penicillin, 50 U/ml streptomycin, 4 mM glutamine, 25 mM HEPES, and 10% FBS. The cells were kept at 37°C in a 5% CO_2 environment. Culture medium was changed every 2 d. Caco-2 cells were subcultured after partial digestion with 0.25% trypsin and 0.9 mM EDTA in Ca^{2+}- and Mg^{2+}-free PBS (11, 23).

Determination of epithelial monolayer resistance and paracellular permeability

An epithelial voltohmmeter (World Precision Instruments, Sarasota, FL) was used for measurements of the transepithelial electrical resistance (TER) of the filter-grown Caco-2 intestinal monolayers as previously reported. The effect of IL-1β on Caco-2 paracellular permeability was determined using an established paracellular marker inulin (molecular mass, 5000 g/mol) (25). For determination of mucosal-to-serosal flux rates of inulin, Caco-2–plated filters having epithelial resistance of 400–500 $\Omega \cdot cm^2$ were used. Known concentrations of inulin (2 μM) and its radioactive tracer were added to the apical solution. Pharmacologic inhibitors were added to Caco-2 monolayers 1 h prior to the IL-1β treatment. The effect of pharmacologic inhibitors on the IL-1β–induced increase in Caco-2 TJ permeability was measured at 48 h following IL-1β treatment. The relative TER in various treatment groups was calculated as a percentage of the control Caco-2 monolayers. The control relative TER was set to 100%.

Assessment of protein expression by Western blot analysis

Caco-2 monolayers were treated with IL-1β (10 ng/ml) for varying time periods. At the end of the experimental period, Caco-2 monolayers were immediately rinsed with ice-cold PBS and cells were lysed with lysis buffer (50 mM Tris-HCl [pH 7.5], 150 mM NaCl, 500 μM NaF, 2 mM EDTA, 100 μM vanadate, 100 μM PMSF, 1 μg/ml leupeptin, 1 μg/ml pepstatin A, 40 mM *para*-nitrophenyl phosphate, 1 μg/ml aprotinin, and 1% Triton X-100) and scraped, and the cell lysates were placed in microcentrifuge tubes. Cell lysates were centrifuged to yield a clear lysate. Supernatant was collected, and protein measurement was performed using a protein assay kit (Bio-Rad Laboratories). Laemmli gel loading buffer was added to the lysate containing 10–20 μg protein and boiled for 7 min, after which proteins were separated on SDS-PAGE gel. Proteins from the gel were transferred to the membrane (Trans-Blot transfer medium, nitrocellulose membrane; Bio-Rad Laboratories) overnight. The membrane was incubated for 2 h in blocking solution (5% dry milk in TBS/Tween 20 buffer). The membrane was incubated with appropriate primary Abs in blocking solution. Concentrations of primary Abs were used according to manufacturers' recommendations (usually 1–2 μg/ml was used). After being washed in TBS/1% Tween 20 buffer, the membrane was incubated in appropriate secondary Abs (1:2000) and developed using the Santa Cruz Western blotting Luminol reagents (Santa Cruz Biotechnology, Santa Cruz, CA) on the Kodak BioMax MS film (Fisher Scientific, Pittsburgh, PA).

siRNA of p38 kinase and ATF-2

Targeted siRNAs were obtained from Dharmacon (Chicago, IL). Caco-2 monolayers were transiently transfected using DharmaFECT transfection reagent (Thermo Scientific, Lafayette, CO) (11). Briefly, 5×10^5 cells per filter were seeded into a 12-well transwell plate and grown to confluency. Caco-2 monolayers were then washed with PBS twice and 0.5 ml Accell medium was added to the apical compartment of each filter and 1.5 ml was added to the basolateral compartment of each filter. Five nanograms of the siRNA of interest and 2 μl DharmaFECT reagent were added in Accell medium to the apical compartment of each filter. The IL-1β experiments were carried out 96 h after transfection. The efficiency of silencing was confirmed by Western blot analysis.

ELISA-based in vitro p38 kinase activity

The p38 kinase activity was carried out using biotinylated ATF-2 coated on streptavidin 96-well plates. The plates were washed three times with PBS, incubated with blocking solution (1 mg/ml BSA in PBS) at 37°C for 1 h, and then washed three times with PBS. The kinase reaction buffer (90 μl) (20 mM Tris-HCl [pH 7.5], 10 mM $MgCl_2$, 50 mM NaCl, 1 mM DTT, 1 mM NaF, 50 μM ATP) provided by the manufacturer (MBL International, Woburn, MA) and the samples containing IL-1β–activated p38 kinase (10 μl) were added to each well, and the kinase reaction (phosphorylation of ATF-2) was carried out at 37°C for 30–60 min. The reaction was stopped by removing the reaction mixtures and washing the plates three times with washing buffer (20 mM Tris-HCl [pH 7.4], 0.5 M NaCl, and 0.05% Tween 20). The washed plates were incubated with the anti–phospho-ATF-2 Ab (10 ng/ml) at room temperature for 1 h. Plates were washed four times with washing buffer, and goat anti-rabbit IgG Ab (diluted at 1:2000 in washing buffer) was added to the wells and the plates were incubated at 37°C for 1 h. The plates were then washed four times and incubated with 100 μl substrate solution tetramethylbenzidine at 37°C for 5–15 min. A stop solution containing 0.5 N H_2SO_4 (100 μl) was added to stop the reaction. The absorbance at 450 nm was determined using the SpectrraMax 190 (Molecular Devices, Sunnyvale, CA).

Nuclear extracts and ELISA for transcription factor ATF-2 activation

Filter-grown Caco-2 monolayers were treated with IL-1β (10 ng/ml) for 30 min. Caco-2 monolayers were washed with ice-cold PBS, scraped, collected, and centrifuged at 14,000 rpm for 30 s. The cell pellets were resuspended in 200 μl buffer A (10 mM HEPES-KOH, 1.5 mM $MgCl_2$, 10 mM KCl, 0.5 mM DTT, and 0.2 mM PMSF [pH 7.9]) and incubated on ice for 15 min. After centrifugation at 14,000 rpm for 30 s, pelleted nuclei were resuspended in 30 μl buffer C (20 mM HEPES-KOH [25% glycerol], 420 mM NaCl, 1.5 mM $MgCl_2$, 0.2 mM EDTA, 0.5 mM DTT, and 0.2 mM PMSF [pH 7.9]). After incubation on ice for 20 min, the lysates were centrifuged at 14,000 rpm for 20 min. Protein concentrations were determined using the Bradford method. The ATF-2 DNA-binding assay was performed using TransAM ELISA-based kits from Active Motif according to the manufacturer's protocol. In brief, the binding reactions contained 1 pM biotinylated probe (Integrated DNA Technologies) and 5 μg nuclear extract in complete binding buffer with a total volume of 50 μl. After 30 min incubation, the solution was transferred to an individual well on a 96-well plate and incubated for 1 h. Appropriate Ab (2 μg/ml) was added to the well to bind the target protein in nuclear extract. After incubation for 1 h, the Ab was removed, and 100 μl HRP-conjugated secondary Ab was added to the well and incubated for 1 h. Subsequently, 100 μl developing solution was added for 2–10 min, and 100 μl stop solution was added. The absorbance at 450 nm was determined using the SpectraMax 190 (Molecular Devices).

Immunostaining of ATF-2

Cellular localization of ATF-2 was assessed by immunofluorescent Ab labeling (26). At the end of the experimental period, filter-grown Caco-2

monolayers were washed twice in cold PBS and were fixed with 2% paraformaldehyde for 20 min. After being permeabilized with 0.1% Triton X-100 in PBS at room temperature for 20 min, Caco-2 monolayers were then incubated in blocking solution composed of BSA and normal donkey serum in PBS for 1 h. Cells were then labeled with primary Ab in blocking solution for 2 h. After being washed with PBS, the cells were incubated in Cy3-conjugated secondary Ab for 1 h at room temperature. ProLong Gold antifade reagent (Invitrogen) was used to mount the filters onto the coverslips. Immunolocalizations of ATF-2 were visualized using a confocal fluorescence microscope (LSM 510; University of New Mexico Imaging Center) equipped with a Hamamatsu digital camera (Hamamatsu Photonics, Hamamatsu, Japan). Images were processed with LSM software (Zeiss, Oberkochen, Germany).

RNA isolation and reverse transcription

Caco-2 cells (5×10^5/filter) were seeded into six-well transwell permeable inserts and grown to confluency. Filter-grown Caco-2 cells were then treated with appropriate experimental reagents for desired time periods. At the end of the experimental period, cells were washed twice with ice-cold PBS. Total RNA was isolated using an RNeasy kit (Qiagen, Valencia, CA) according to the manufacturer's protocol. Total RNA concentration was determined by absorbance at 260/280 nm using a SpectraMax 190 (Molecular Devices). The reverse transcription (RT) was carried out using the GeneAmp Gold RNA PCR core kit (Applied Biosystems, Foster City, CA). Two micrograms total RNA from each sample was reverse transcribed into cDNA in a 40-μl reaction containing 1× RT-PCR buffer, 2.5 mM $MgCl_2$, 250 μM of each dNTP, 20 U RNase inhibitor, 10 mM DTT, 1.25 μM random hexamer, and 30 U multiscribe RT. The RT reactions were performed in a thermocycler (MyCycler; Bio-Rad, Hercules, CA) at 25°C for 10 min, 42°C for 30 min, and 95°C for 5 min.

Quantification of gene expression using real-time PCR

The real-time PCRs were carried out using an ABI prism 7900 sequence detection system and a TaqMan Universal PCR Master Mix kit (Applied Biosystems, Branchburg, NJ) as previously described (27). Each real-time PCR reaction contained 10 μl RT reaction mix, 25 μl 2× TaqMan Universal PCR Master Mix, 0.2 μM probe, and 0.6 μM primers. Primer and probe design for the real-time PCR was made with Primer Express version 2 from Applied Biosystems. The primers used in this study are as follows: MLCK specific primer pairs consisted of 5′-AGGAAGGCAGCATTGAGGTTT-3′ (forward), 5′-GCTTTCAGCAGGCAGAGGTAA-3′ (reverse); probe specific for MLCK consisted of FAM-5′-TGAAGATGCTGGCTCC-3′-TAMRA; the internal control GAPDH-specific primer pairs consisted of 5′-CCACCCATGGCAAATTCC-3′ (forward), 5′-TGGGATTTCCATTGATGACCAG-3′ (reverse); probe specific for GAPDH consisted of JOE-5′-TGGCACCGTCAAGGCTGAGAACG-3′-TAMRA. All runs were performed according to the default PCR protocol (50°C for 2 min, 95°C for 10 min, 40 cycles of 95°C for 15 s, and 60°C for 1 min). For each sample, real-time PCR reactions were performed in triplicate, and the average threshold cycle was calculated. A standard curve was generated to convert the threshold cycle to copy numbers. Expression of MLCK mRNA was normalized with GAPDH mRNA expression. The average copy number of MLCK mRNA expression in control samples was set to 1.0. The relative expression of MLCK mRNA in treated samples was determined as a fold increase compared with control samples.

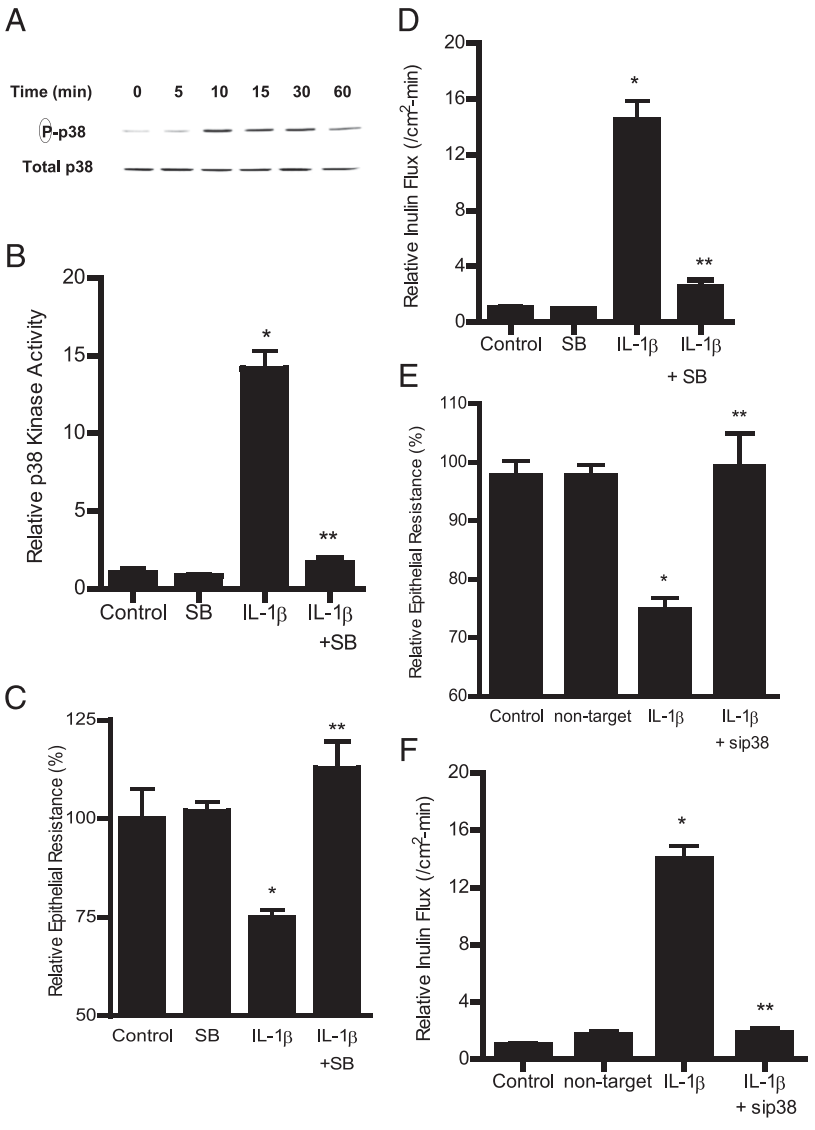

FIGURE 1. Effect of IL-1β on p38 kinase activation in filter-grown Caco-2 monolayers. (**A**) IL-1β (10 ng/ml) caused a time-dependent increase in phosphorylated p38 kinase (total p38 was used for equal protein loading). (**B**) IL-1β caused an increase in p38 kinase activity as determined by ELISA-based in vitro kinase activity. Pretreatment with p38 kinase inhibitor SB-203580 (10 μM) 1 h prior to IL-1β treatment prevented the IL-1β–induced increase in p38 kinase activity. *$p < 0.001$ versus control, **$p < 0.001$ versus IL-1β ($n = 4$). (**C**) SB-203580 prevented the IL-1β–induced drop in Caco-2 TER for the 48-h experimental period ($n = 6$). *$p < 0.001$ versus control, **$p < 0.001$ versus IL-1β. (**D**) pretreatment with SB-203580 (10 μM) prevented the IL-1β increase in mucosal-to-serosal inulin flux for the 48-h experimental period ($n = 6$). *$p < 0.001$ versus control, **$p < 0.001$ versus IL-1β treatment. (**E**) p38 kinase siRNA transfection (96-h period) prevented the IL-1β–induced drop in Caco-2 TER for the 48-h experimental period ($n = 6$). (**F**) p38 kinase siRNA transfection prevented the IL-1β–induced increase in inulin flux for the 48-h experimental period ($n = 6$). *$p < 0.001$ versus control, **$p < 0.001$ versus IL-1β treatment.

Transfection of MLCK DNA and measurement of promoter activity

The MLCK promoter region was cloned using the GenomeWalker system (Clontech Laboratories, Mountain View, CA). A 2091-bp DNA fragment (−2109 to −18) was amplified by PCR (27). The amplification condition was 1 cycle at 94°C for 2 min, followed by 43 cycles at 94°C for 1 min, 50°C for 1 min, and 72°C for 2 min and 1 cycle at 72°C for 5 min. The resultant PCR product was digested with HindIII and KpnI and inserted into pGL3-basic luciferase reporter vector (Promega). The sequence was confirmed by DNA services at the University of New Mexico. MLCK promoter was transiently transfected into Caco-2 cells using transfection reagent Lipofectamine 2000 (Life Technologies). *Renilla* luciferase vector (pRL-TK; Promega) was cotransfected with each plasmid construct as an internal control. Cells (5×10^5/filter) were seeded into a six-well transwell plate and grown to confluency. Caco-2 monolayers were then washed with PBS twice and 1.0 ml Opti-MEM medium was added to the apical compartment of each filter and 1.5 ml was added to the basolateral compartment of each filter. One microgram of each plasmid construct and 0.25 μg pRL-TK or 2 μl Lipofectamine 2000 were preincubated in 250 μl Opti-MEM, respectively. After 5 min incubation, two solutions were mixed and incubated for another 20 min, and the mixture was added to the apical compartment of each filter. After incubation for 3 h at 37°C, 500 μl DMEM containing 10% FBS was added to both sides of the filter to reach a 2.5% final concentration of FBS. Subsequently, media were replaced with normal Caco-2 growth media 16 h after transfection. Specific experiments were carried out 48 h after transfection. At the completion of specific experimental treatments, Caco-2 cells were washed twice with 1 ml ice-cold PBS, followed by the addition of 400 μl 1× passive lysis buffer, incubated at room temperature for 15 min, scraped and transferred into an Eppendorf tube, and centrifuged for 15 s at 13,000 rpm in a microcentrifuge. Luciferase activity was determined using the dual luciferase assay kit (Promega). Twenty microliters of the supernatant was used for each assay. Luciferase values were determined by Lumat LB 9507 luminometer (EG&G Berthold, Oak Ridge, TN). The values of reporter luciferase activities were then divided by those of *Renilla* luciferase activities to normalize for differences in transfection efficiencies. The average activity value of the control samples was set to 1.0. The luciferase activity of MLCK promoter in treated samples was determined relative to the control samples.

In vivo mouse intestinal permeability measurements

The Laboratory Animal Care and Use Committee at the University of New Mexico approved all experimental protocols. The mouse intestinal permeability was measured by recycling small intestinal perfusion as previously described (28–31). After the experimental period, mice were anesthetized with isoflurane. After midline incision of the abdomen, 5 cm intestine segment was isolated and cannulated at the proximal and distal ends with 0.76-mm internal diameter polyethylene tubing. Flushing solution (140 mM NaCl, 10 mM HEPES [pH 7.4]) warmed to 37°C was first perfused through the intestine at 1 ml/min for 20 min followed by air flush to remove residual contents using an external pump (Bio-Rad Laboratories). This was followed by perfusion of 5 ml perfusate solution (85 mM

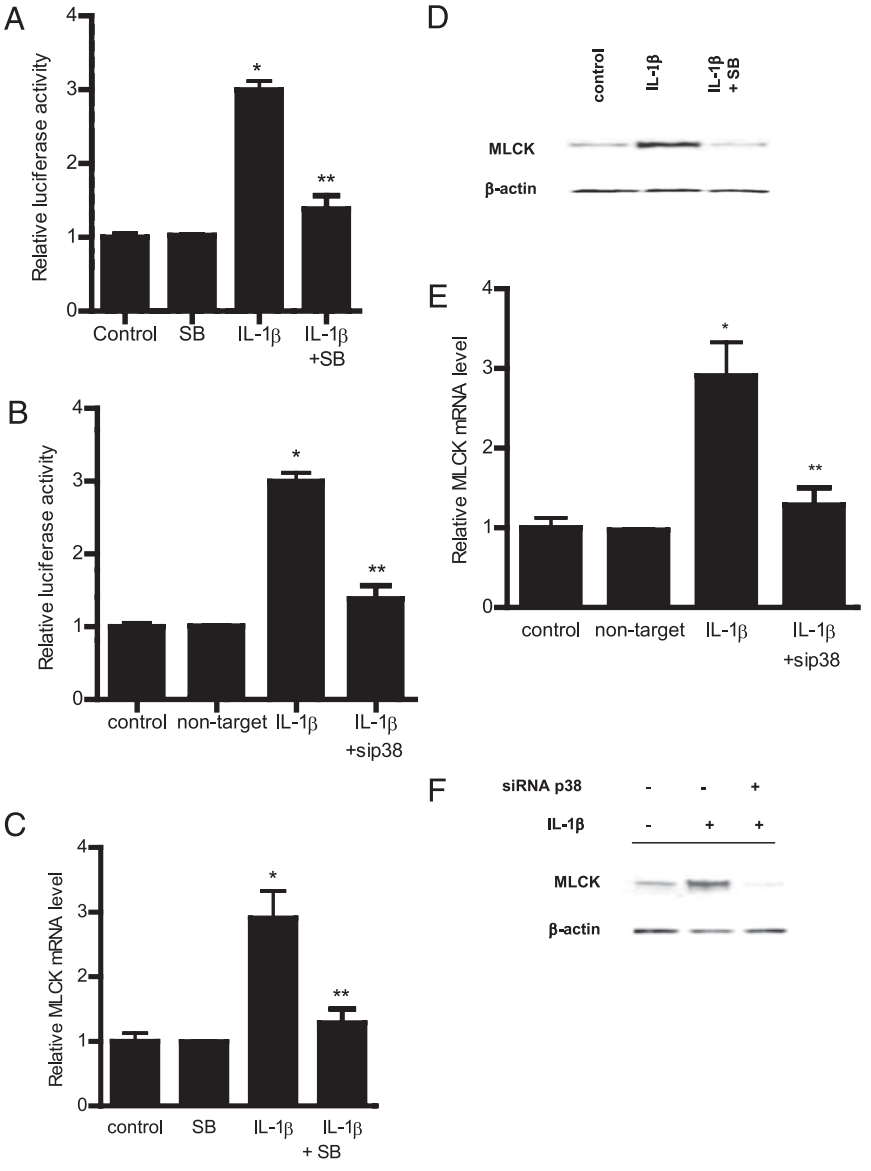

FIGURE 2. Effect of p38 kinase inhibition on IL-1β induced increase in MLCK gene and protein expression. (**A**) Pretreatment with p38 kinase inhibitor SB-203580 1 h prior to IL-1β treatment prevented the IL-1β–induced increase in Caco-2 MLCK promoter activity as assessed by luciferase assay in the 4-h experimental period ($n = 8$). *$p < 0.0001$ versus control, **$p < 0.0001$ versus IL-1β treatment. (**B**) p38 kinase knockdown by siRNA transfection prevented the IL-1β–induced increase in MLCK promoter activity as assessed by luciferase activity in the 4-h experimental period ($n = 8$). Caco-2 monolayers were cotransfected with siRNA p38 kinase for 96 h before IL-1β treatment. *$p < 0.0001$ versus control, **$p < 0.0001$ versus IL-1β treatment. (**C**) Pretreatment with p38 kinase inhibitor SB-203580 1 h prior to IL-1β treatment prevented the increase in MLCK mRNA levels in the 6-h experimental period ($n = 8$). MLCK mRNA level was expressed relative to the control level, which was assigned a value of 1. The average copy number of MLCK mRNA in controls was 4.63×10^{11}. *$p < 0.001$ versus control, **$p < 0.001$ versus IL-1β treatment. (**D**) IL-1β treatment caused an increase in Caco-2 MLCK protein expression as assessed by Western blot analysis in the 48-h experimental period ($n = 3$). Pretreatment with p38 kinase inhibitor SB-203580 1 h prior to IL-1β treatment prevented the increase in MLCK protein expression. (**E**) siRNA-induced knockdown of p38 kinase prevented the IL-1β–induced increase in MLCK mRNA in the 6-h experimental period ($n = 8$). *$p < 0.001$ versus control, **$p < 0.001$ versus IL-1β treatment. (**F**) siRNA induced knockdown of p38 kinase prevented the IL-1β–induced increase in MLCK protein levels. Caco-2 monolayers were cotransfected with siRNA p38 kinase for 96 h before IL-1β treatment.

NaCl, 10 mM HEPES, 20 mM sodium ferrocyanide, 5 mM KCl, 5 mM $CaCl_2$ [pH 7.4]) containing Texas Red–labeled dextran (10 kDa) in a recirculating manner at 0.75 ml/min for 2 h. The abdominal cavity was covered with moistened gauze, and body temperature was measured via rectal thermometer, and temperature was maintained at 37.5 ± 0.5°C using a heating lamp. One-milliliter aliquots of test solution were removed at the beginning and end of the perfusion. After perfusion, the animal was sacrificed and the perfused intestine segment was excised and the length measured. The excised intestinal tissue was then snap-frozen in optimal cutting temperature compound or used for protein and RNA analysis. Ferrocyanide concentration in the perfusate was measured using colorimetric assay. Texas Red–labeled dextran (10 kDa) concentration was measured using an excitation wavelength of 595 nm and an emission wavelength of 615 nm in a microplate reader. Probe clearance was calculated as $C_{probe} = (C_i V_i - C_f V_f)/(C_{avg} TL)$. In the equation, C_i represents the measured initial probe concentration; C_f represents the measured final probe concentration; V_i represents the measured initial perfusate volume; V_f was calculated as $V_i([\text{ferrocyanide}]_i/[\text{ferrocyanide}]_f)$; C_{avg} was calculated as $(C_i - C_f)/\ln(C_i/C_f)$; T represents hours of perfusion; and L represents the length of the perfused intestine section in centimeters.

Animal surgery and in vivo transfection of p38 and ATF-2 siRNA

Mice were fasted for 24 h prior to the surgery. Mice were anesthetized with isoflurane (4% for surgical induction, 1% for maintenance) using oxygen as carrier during surgical procedures. Surgical procedures were performed using sterile technique. The abdomen was opened by a midline incision, and a 6-cm intestine segment was isolated at the proximal and distal ends and tied with sutures. siRNA transfection solution (0.5 ml; containing Accell medium, 2.5 nmol p38 or ATF-2 siRNA, and 50 μl transfecting agent Lipofectamine) was introduced into the isolated intestine segment (surface area 6 cm^2) for a 1-h transfection period. Control animals underwent sham operation, where the siRNA transfection solution contained Accell medium, 2.5 nmol nontarget siRNA, and 50 μl transfecting agent Lipofectamine. The abdominal cavity was covered with moistened gauze. Body temperature was monitored continuously with a rectal probe and maintained at 37.5 ± 0.5°C using a heating pad. After a 1-h transfection period, each end of the intestinal segment was untied, the intestine was placed back in the abdominal cavity, and the abdomen was closed. Three days following transfection, functional studies of the intestinal epithelial barrier were performed. The surgery and the in vivo transfection procedures had no effect on the food intake and the body weight of the animals during the experimental period. The average animal weight averaged between 23 and 25 g during the experimental period.

Statistical analysis

Statistical significance of differences between mean values was assessed with Student t tests for unpaired data and ANOVA analysis whenever required. All reported significance levels represent two-tailed p values. A p value <0.05 was used to indicate statistical significance. All in vitro experiments using Caco-2 monolayers, including assessment of TJ barrier, biochemical and molecular studies, and kinase activity measurements, were carried out in triplicates or quadruplicates and repeated at a minimum of three times for reproductivity. The immunoblot analysis and cell imaging studies were repeated three to four times. The animal studies were carried out individually and each experimental group consisted of $n = 3$–6 animals.

Results

Role of p38 kinase pathway in IL-1β–induced increase in Caco-2 intestinal epithelial TJ permeability

In the following studies, we examined the involvement of the p38 kinase pathway in IL-1β–induced increase in Caco-2 intestinal epithelial TJ permeability. The effect of IL-1β on p38 kinase activation was determined by p38 kinase phosphorylation and by in vitro kinase assays of p38 kinase. IL-1β at physiological concentration (10 ng/ml) caused a time-dependent increase in p38 kinase phosphorylation in filter-grown Caco-2 monolayers (Fig. 1A). IL-1β (10 ng/ml) caused an increase in p38 kinase phosphorylation by 10 min of treatment, and the increase persisted up to 30 min as determined by phospho–p38 kinase immunoblotting (Fig. 1A). The total p38 kinase levels were not affected by the IL-1β treatment (Fig. 1A). The IL-1β effect on kinase activity of immunoprecipitated p38 kinase was also determined directly by an ELISA-based in vitro kinase assay. Following IL-1β treatment, p38 kinase was immunoprecipitated and kinase activity measured in vitro using ATF-2 as the substrate as described in *Materials and Methods*. IL-1β caused an increase in p38 kinase activity, and addition of p38 kinase inhibitor SB-203580 (10 μM) inhibited the increase in p38 kinase activity (Fig. 1B). These results suggested that IL-1β induces a rapid phosphorylation and activation of p38 kinase in Caco-2 cells. Next, to determine whether p38 kinase activation was required for the IL-1β–induced increase in Caco-2 TJ permeability, the effect of p38 kinase inhibition was examined. The IL-1β effect on Caco-2 TJ permeability was measured by assessing TER and transepithelial flux of the paracellular marker inulin (11, 32). IL-1β caused a drop in Caco-2 TER and an increase in paracellular permeability (Fig. 1C, 1D). The p38 kinase inhibitor SB-203580 prevented the IL-1β–induced drop in Caco-2 TER (Fig. 1C) and increase in inulin flux (Fig. 1D), suggesting that p38 kinase activation was required for the increase in Caco-2 TJ permeability. The IL-1β effect on TJ permeability was also assessed in other cell types including HT-29 and T84 intestinal cell lines and the Madin-Darby canine kidney (MDCK) cell line. In these studies, IL-1β caused a dose-dependent decrease in TER in HT-29, T-84, and MDCK monolayers (data not shown). These data suggested that the IL-1β effect was a generalized phenomenon.

To further validate the requirement of p38 kinase in the IL-1β effect on Caco-2 TJ permeability, p38 kinase expression was

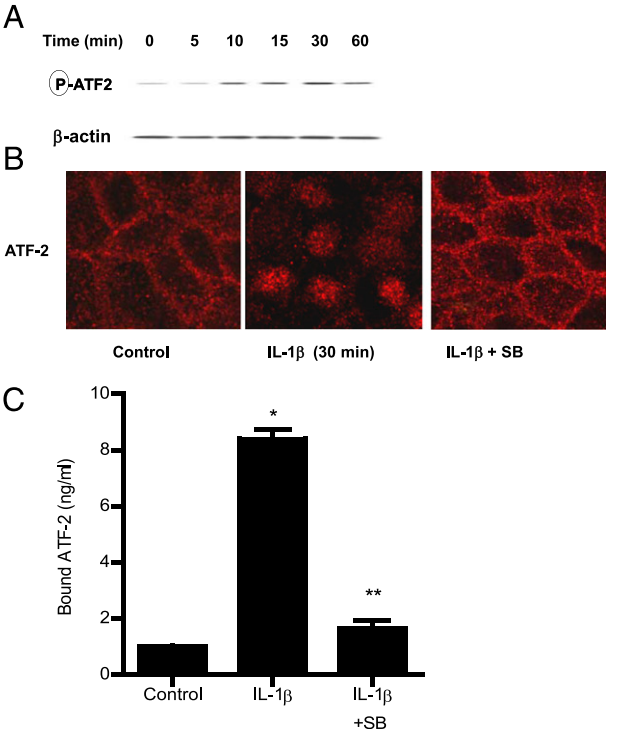

FIGURE 3. Effect of IL-1β on ATF-2 activation. (**A**) IL-1β (10 ng/ml) caused a time-dependent increase in ATF-2 phosphorylation as assessed by Western blot analysis ($n = 3$). (**B**) IL-1β treatment resulted in ATF-2 cytoplasmic-to-nuclear translocation as determined by immunofluorescent Ab labeling as described in *Materials and Methods* (30-min experimental period) ($n = 3$). Pretreatment with p38 kinase inhibitor SB-203580 1 h prior to IL-1β treatment prevented the IL-1β–induced ATF-2 nuclear translocation. Original magnification ×40. (**C**) Pretreatment with p38 kinase inhibitor SB-203580 1 h prior to IL-1β treatment prevented the IL-1β–induced binding of ATF-2 to its binding site on DNA probe as measured by DNA ELISA binding assay ($n = 6$). *$p < 0.001$ versus control, **$p < 0.001$ versus IL-1β treatment.

silenced by p38 kinase siRNA transfection of Caco-2 monolayers. The p38 kinase siRNA transfection resulted in a nearly complete knockdown of p38 kinase (data not shown), and siRNA knockdown of p38 prevented the IL-1β–induced drop in Caco-2 TER (Fig. 1E) and increase in inulin flux (Fig. 1F), confirming the requirement of p38 kinase.

p38 kinase pathway regulation of Caco-2 MLCK gene activity

Previous studies from our laboratory suggested that the IL-1β–induced increase in Caco-2 TJ permeability was mediated by MLCK gene activation and transcription (23, 24). In the following studies, we examined the possibility that the p38 kinase pathway regulates the MLCK gene activity. The IL-1β effect on MLCK gene activity was determined by assessing MLCK promoter activity and mRNA expression. In these studies, MLCK promoter activity was determined by measuring luciferase activity (reporter gene) following transfection of filter-grown Caco-2 monolayers with a plasmid vector containing the MLCK promoter region (24). IL-1β caused a significant increase in MLCK promoter activity as assessed by the luciferase assay (Fig. 2A), and inhibition of p38 kinase by SB-203580 prevented the increase in MLCK promoter activity (Fig. 2A). Additionally, siRNA-induced knockdown of p38 kinase also inhibited the IL-1β–induced increase in MLCK promoter activity (Fig. 2B). These results indicated that the IL-1β–induced increase in MLCK promoter activity required p38 kinase activation. In the following series of studies, the role of the p38 kinase pathway in IL-1β increases in MCLK mRNA and protein expression was also examined. Consistent with the MLCK promoter studies, IL-1β treatment resulted in an increase in Caco-2 MLCK mRNA and protein levels (Fig. 2C, 2D). In previous time-course studies, we showed that IL-1β causes a peak increase in MLCK mRNA expression at 4–6 h and a peak increase in MLCK protein expression and activity at the 24–48 h time point (23). As shown above, IL-1β caused a rapid activation of p38 kinase (within minutes of IL-1β treatment). The addition of the p38 kinase inhibitor SB-208530 (10 μM) inhibited the IL-1β increase in MLCK mRNA and protein levels in Caco-2 cells (Fig. 2C, 2D). The siRNA-induced knockdown of p38 kinase also inhibited the increase in MLCK mRNA and protein (Fig. 2E, 2F). Taken together, these data suggested that the IL-1β–induced increase in MLCK promoter activity and mRNA expression required p38 kinase activation.

Role of ATF-2 in IL-1β modulation of MLCK gene activity and Caco-2 TJ permeability

In the following studies, the molecular processes that regulate the p38 kinase pathway activation of MLCK promoter activity and Caco-2 TJ permeability were examined. Previous studies have shown nuclear transcription factor, ATF-2, to be a direct substrate of p38 kinase (33). The IL-1β effect on ATF-2 activation was examined by measuring ATF-2 phosphorylation and cytoplasmic-to-nuclear translocation and by using a DNA binding assay. IL-1β caused a time-dependent increase in Caco-2 ATF-2 phosphorylation, starting at ~10 min of treatment (Fig. 3A). IL-1β also caused a cytoplasmic-to-nuclear translocation of activated ATF-2 in Caco-2 monolayers (Fig. 3B) and an increase in binding of ATF-2 (in the nuclear fraction) to the ATF-2 binding sequence on the DNA probe (Fig. 3C). The addition of the p38 kinase inhibitor

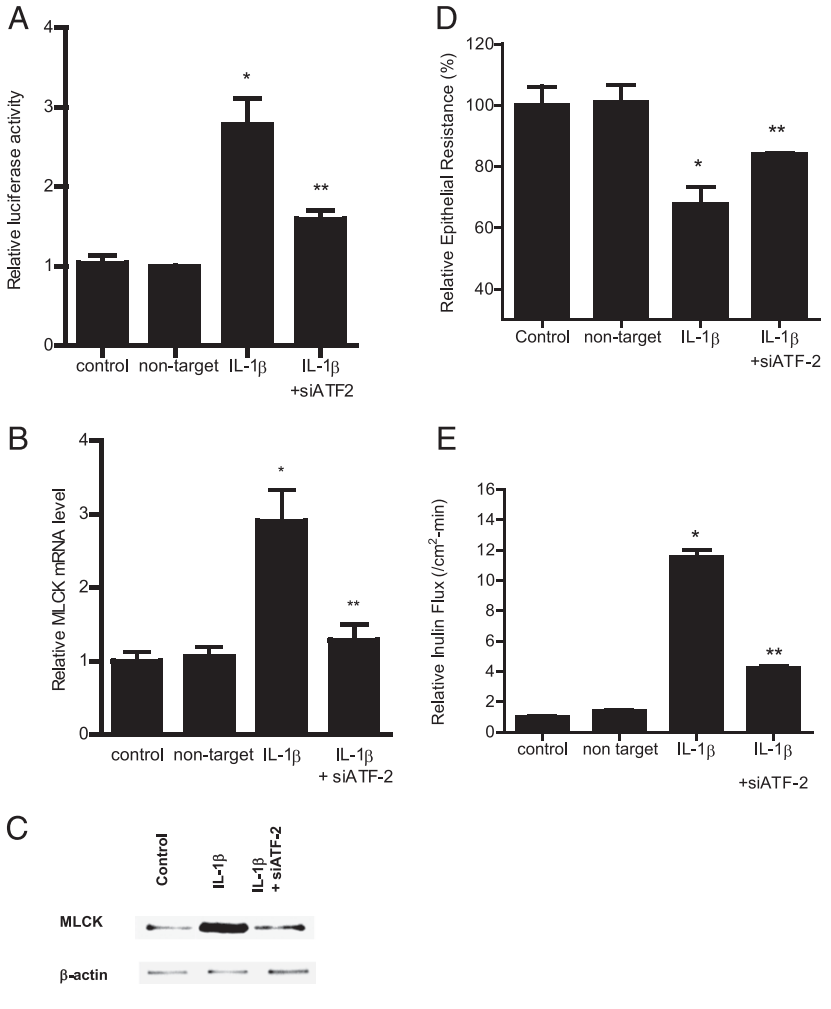

FIGURE 4. Effect of siRNA-induced ATF-2 knockdown on IL-1β–induced increase in Caco-2 MLCK expression. (**A**) ATF-2 siRNA transfection significantly prevented the IL-1β–induced increase in Caco-2 MLCK promoter activity as assayed by luciferase assay in the 4-h experimental period ($n = 8$). $*p < 0.001$ versus control, $**p < 0.001$ versus IL-1β treatment. (**C**) ATF-2 siRNA transfection inhibited the IL-1β–induced increase in Caco-2 MLCK mRNA levels in the 6-h experimental period ($n = 8$). $*p < 0.001$ versus control, $**p < 0.001$ versus IL-1β treatment. (**D**) ATF-2 siRNA transfection prevented the IL-1β–induced increase in Caco-2 MLCK protein expression in the 48-h experimental period ($n = 3$). (**E**) ATF-2 siRNA transfection prevented the IL-1β–induced drop in Caco-2 TER in the 48-h experimental period ($n = 6$). $*p < 0.001$ versus control, $**p < 0.001$ versus IL-1β treatment. (**B**) ATF-2 silencing inhibited the IL-1β increase in mucosal-to-serosal inulin flux in the 48-h experimental period ($n = 6$). $*p < 0.0001$ versus control, $**p < 0.0001$ versus IL-1β treatment. Caco-2 monolayers were cotransfected with siRNA ATF-2 for 96 h before IL-1β treatment.

SB-203580 inhibited the phosphorylation, cytoplasmic-to-nuclear translocation, and DNA binding of ATF-2 (Fig. 3B, 3C). These results suggested that p38 kinase induces the phosphorylation, cytoplasmic-to-nuclear translocation, and DNA binding of ATF-2. Next, the regulatory role of ATF-2 on MLCK promoter activity was examined by siRNA silencing of ATF-2 in Caco-2 monolayers. The transfection of filter-grown Caco-2 monolayers with ATF-2 siRNA caused a depletion of ATF-2 expression (data not shown). The siRNA knockdown of ATF-2 resulted in an inhibition of the IL-1β increase in MLCK promoter activity (Fig. 4A), suggesting that ATF-2 mediates the upregulation of MLCK promoter activity. Additionally, the siRNA knockdown of ATF-2 also inhibited the IL-1β increase in MLCK mRNA and protein level (Fig. 4B, 4C) and the IL-1β–induced drop in Caco-2 TER (Fig. 4D) and increase in inulin flux (Fig. 4E). Taken together, these data suggested that ATF-2 activation was required for the increase in MLCK gene activity and Caco-2 TJ permeability.

Molecular determinants that mediate ATF-2 regulation of MLCK promoter activity

To further examine the molecular processes involved, the molecular determinants that mediate ATF-2 regulation of MLCK promoter activity were investigated. Using Genomatix Promoter Inspector software, potential ATF-2 binding sequences were identified on the full-length MLCK promoter region (2091 bp); only one ATF-2 binding motif was identified on the MLCK promoter region, which was located between −268 and −259 (AGCCACCCAT) (Fig. 5A) within the minimal promoter region (24). The binding of IL-1β–activated ATF-2 to the ATF-2 binding motif on MLCK promoter region was determined by an ELISA-based DNA binding assay. A 50-bp oligonucleotide probe encoding the promoter region containing the ATF-2 binding motif was synthesized (11, 27). IL-1β treatment of Caco-2 cells resulted in an increased binding of ATF-2 to the DNA probe (Fig. 5B). The mutation of the ATF-2 binding site prevented the ATF-2 binding (Fig. 5B). To further validate the role of the ATF-2 binding sequence in MLCK promoter activity, the ATF-2 binding site on the full-length MLCK promoter region was also mutated via a site-directed mutagenesis. The mutation of the ATF-2 binding site (AGCCACCCAT → GATTGTTTGC) inhibited the IL-1β increase in MLCK promoter activity (Fig. 5C). These data indicated that the p38 kinase pathway regulation of MLCK promoter activity was mediated by ATF-2 binding to the AGCCACCCAT nucleotide sequence on the MLCK promoter region.

Role of p38 kinase and ATF-2 in IL-1β–induced increase in intestinal permeability in vivo

The above studies suggested that the p38 kinase pathway and ATF-2 activation played an integral role in the IL-1β modulation of MLCK gene and TJ permeability in filter-grown Caco-2 monolayers; however, the in vivo relevance of these findings remain unclear. Thus, in the following studies, the in vivo relevance of the p38 kinase pathway and ATF-2 activation in IL-1β modulation of mouse intestinal permeability was examined by in vivo intestinal perfusion of mouse small intestine (31). The i.p. injection of IL-1β (5 μg) caused an increase in intestinal permeability as assessed by mucosal-to-serosal flux of commonly used paracellular marker Texas Red–labeled dextran (10 kDa) (Fig. 6A). IL-1β treatment resulted in a time-dependent increase in p38 kinase and ATF-2 phosphorylation in the intestinal tissue (Fig. 6B). The increase in

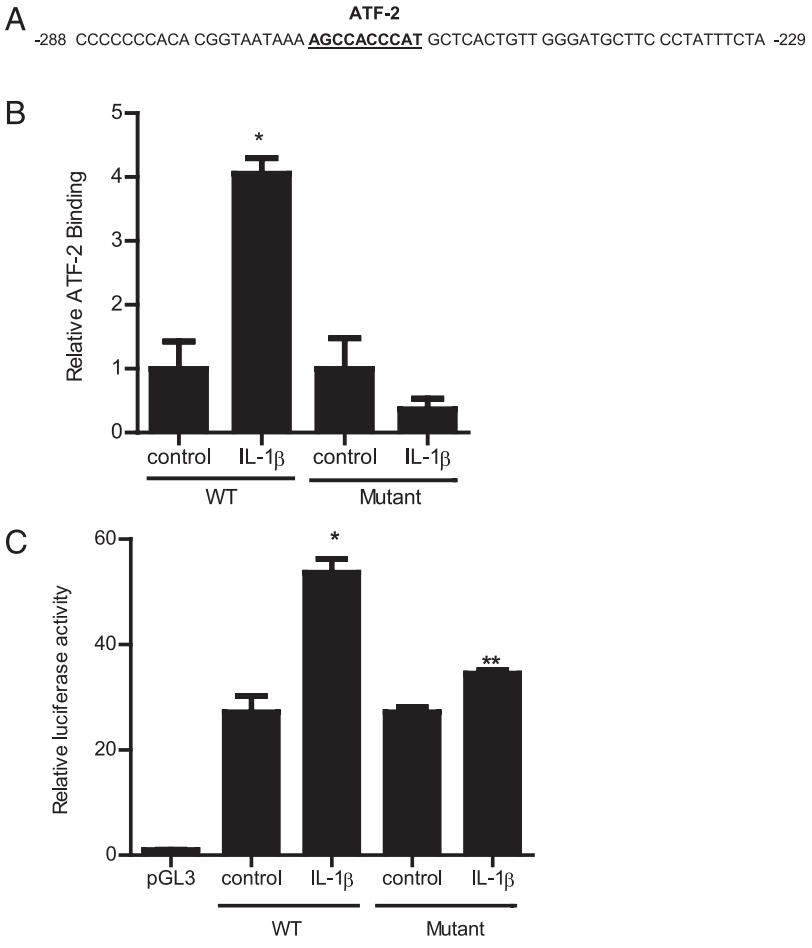

FIGURE 5. (**A**) ATF-2 binding sequence on the MLCK promoter region. Partial 60-bp sequence of the MLCK promoter region encoding the ATF-2 binding motif (−268 to −259) is shown (binding sequence is underlined). (**B**) IL-1β treatment of Caco-2 cells resulted in increased binding of ATF-2 to its binding site on the wild-type (WT) DNA probe encoding the ATF-2 binding region on MLCK promoter as determined by ELISA-based DNA binding assay in the 30-min experimental period ($n = 6$). Oligonucleotide probe with the mutation of the ATF-2 binding site did not cause an increase in ATF-2 binding following IL-1β treatment in the 30-min experimental period ($n = 6$). *$p < 0.0001$ versus control. WT probe, 5′-GGTAATAAAAGCCACCCATCGTCACTGTTGGGATGCTTCCCTATTTCTA-3′; mutant probe, 5′-GGTAATAAAGATTGTTTGCTACTGTCACCAGGATGCTTCCCTATTTCTA-3′. (**C**) Site-directed mutagenesis of ATF-2 binding site (AGCCACCCAT) on the full-length (2091-bp) MLCK promoter prevented the IL-1β–induced increase in MLCK promoter activity in the 4-h experimental period ($n = 8$). *$p < 0.001$ versus control.

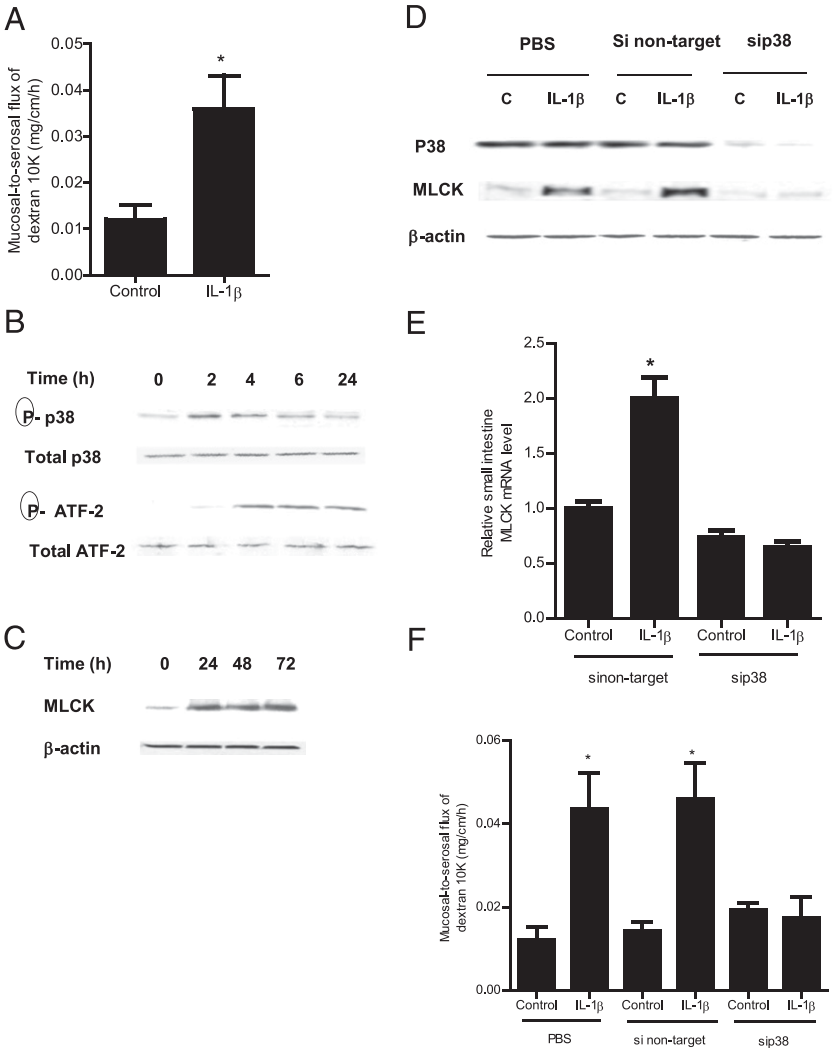

FIGURE 6. Effect of IL-1β on p38 kinase signaling pathway in mouse small intestinal tissue in vivo. (**A**) IL-1β (5 μg) caused an increase in mouse intestinal mucosal-to-serosal flux of dextran (10 kDa) in the 24-h experimental period ($n = 6$). *$p < 0.005$ versus control. (**B**) IL-1β caused a time-dependent and sequential increase in phosphorylated p38 kinase and ATF-2 (total p38 and total ATF-2 were used for equal protein loading) ($n = 3$). (**C**) IL-1β caused a time-dependent increase in mouse MLCK protein expression as assessed by Western blot analysis ($n = 3$). (**D**) p38 kinase siRNA transfection prevented the IL-1β–induced increase in mouse intestinal MLCK protein expression in the 24-h experimental period ($n = 3$). (**E**) p38 kinase siRNA transfection inhibited the IL-1β–induced increase in mouse MLCK mRNA levels in the 24-h experimental period ($n = 4$). *$p < 0.001$ versus control. (**F**) p38 kinase silencing inhibited the IL-1β increase in mucosal-to-serosal flux of dextran (10 kDa) in the 24-h experimental period ($n = 4$). *$p < 0.0001$ versus control.

p38 kinase phosphorylation preceded the ATF-2 phosphorylation. IL-1β also caused an increase in MLCK mRNA and protein expression in the intestinal tissue (Fig. 5C, 5E). To confirm the regulatory action of the p38 kinase pathway in intestinal MLCK expression and intestinal permeability in vivo, intestinal p38 expression was silenced by in vivo siRNA transfection using a recently introduced methodology (29, 31). In brief, 6 cm mouse jejunum was isolated using sutures and the mucosal surface was exposed to transfection solution containing p38 kinase siRNA for 1 h; the sutures were removed and the intestinal segment reinserted into the original location in the abdomen and the abdominal cavity was closed with sutures. After 2 d, mice were treated with IL-1β and intestinal permeability studies were performed on day 3. As shown in Fig. 6D, in vivo p38 siRNA transfection resulted in a nearly complete knockdown of p38 kinase in the intestinal tissue. The siRNA transfection affected the whole intestinal tissue. Moreover, the siRNA knockdown of p38 prevented the IL-1β–induced increase in intestinal tissue MLCK expression (Fig. 6D, 6E) and intestinal permeability (Fig. 6F), confirming the requirement of p38 kinase in the IL-1β–induced increase in MLCK gene expression and intestinal permeability in vivo. Next, the effect of siRNA-induced silencing of ATF-2 on MLCK gene expression and intestinal permeability was examined. The siRNA-induced knockdown of ATF-2 in vivo (Fig. 7A) prevented the IL-1β–induced increase in mouse intestinal tissue MLCK protein and mRNA expression and intestinal permeability (Fig. 7A–C). Additionally, the siRNA-induced knockdown of p38 kinase prevented the increase in ATF-2 phosphorylation, confirming that p38 kinase activation was required for the intestinal tissue ATF-2 activation in vivo (Fig. 7D). Taken together, these data indicated that the IL-1β–induced increase in mouse intestinal permeability in vivo was also mediated by p38 kinase activation of ATF-2 and an ATF-2–dependent increase in MLCK gene expression.

Discussion

The defective intestinal TJ barrier is an important pathogenic factor contributing to the development of intestinal inflammation by allowing increased bacterial Ag penetration (1, 2, 4). IL-1β levels are markedly elevated in inflammatory bowel disease (IBD) and play a central role in the inflammatory process (9–11, 15, 20). In addition to its direct effects on immune activation, IL-1β also causes an increase in intestinal TJ permeability (11, 20). Previous studies from our laboratory suggested that the IL-1β modulation of the intestinal TJ barrier was dependent on MLCK gene activation (19). In this study, we extend our previous findings to delineate the role of the p38 kinase signaling cascade in mediating the IL-1β regulation of the MLCK gene and intestinal permeability.

The p38 kinase pathway has been shown to play an important role in mediating some of the IL-1β–induced immune responses (34, 35). The p38 kinase pathway is known to regulate wide-ranging proinflammatory responses, including stimulation of

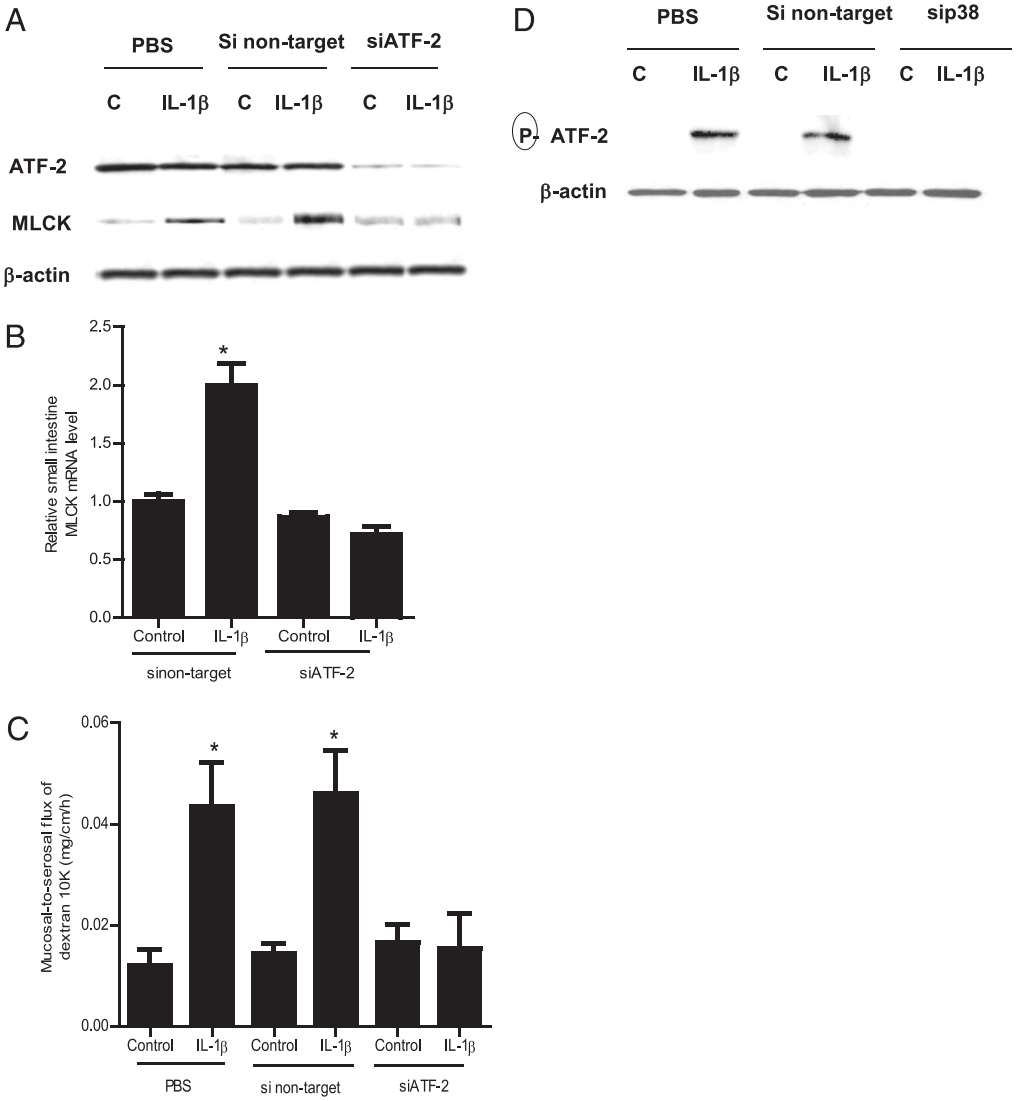

FIGURE 7. Effect of siRNA-induced ATF-2 knockdown on IL-1β–induced increase in mouse intestinal MLCK expression and mouse intestinal permeability. (**A**) ATF-2 siRNA transfection resulted in a nearly complete depletion in mouse intestinal ATF-2 protein expression. ATF-2 siRNA transfection prevented the IL-1β–induced increase in mouse intestinal MLCK protein expression in the 24-h experimental period ($n = 3$). (**B**) ATF-2 siRNA transfection inhibited the IL-1β–induced increase in mouse MLCK mRNA levels in the 24-h experimental period ($n = 3$). *$p < 0.001$ versus control. (**C**) ATF-2 silencing inhibited the IL-1β increase in mucosal-to-serosal flux of dextran (10 kDa) in the 24-h experimental period ($n = 3$). *$p < 0.0001$ versus control. (**D**) siRNA-induced knockdown of p38 kinase prevented the IL-1β–induced activation (phosphorylation) of ATF-2 in mouse intestinal tissue in the 4-h experimental period ($n = 3$).

proinflammatory genes (36, 37), induction of COX-2 (38), increases in iNOS expression (39), increases in adhesion molecule expression (40–42), and proliferation of inflammatory cells (43–46). The p38 kinase is both upregulated and activated in intestinal tissue of patients with IBD, and inhibition of p38 kinase inhibits the secretion of inflammatory cytokines in intestinal tissue and in lamina propria mononuclear cells isolated from IBD patients (47, 48). Previous studies have suggested that p38 kinase may also be involved in TJ barrier regulation (49). Some suggested that p38 kinase may lead to an increase in TJ permeability, whereas others found the opposite to be the case (49–53). Wang et al. (49) reported that the p38 kinase inhibitor SB-203580 inhibited the cytokine mixture (TNF-α, IFN-γ, and IL-1β)–induced increase in Caco-2 TJ permeability. In contrast, p38 kinase caused an enhancement of endothelial TJ barrier (54). Campbell et al. (54) found that the endostatin-induced increase in occludin expression and enhancement of the TJ barrier in retinal endothelial cells required an activation of the p38 kinase pathway. Although these studies suggested that the p38 kinase pathway may have a role in TJ barrier regulation, their precise involvement and the mechanism of action remained unclear.

The involvement of MLCK in TJ barrier regulation has been firmly established by studies from our laboratory and by others (23, 24, 28). It has been shown that the overexpression of constitutively active MLCK in MDCK cells results in an increase in MDCK TJ permeability (55). Additionally, MLCK was shown to play a central role in cytochalasin, alcohol, and low calcium solution–induced increase in Caco-2 TJ permeability (56–58). The increase in Caco-2 TJ permeability required an increase in MLCK activity, and MLCK inhibitors prevented the increase in Caco-2 TJ permeability (56–58). Similarly, the Na^+-glucose cotransport–induced increase in Caco-2 TJ permeability also required an increase in MLCK activity (30). The increase in MLCK activity induces the contraction of perijunctional actomyosin filaments, leading to a mechanical tension–induced opening of the TJ barrier (58, 59). Recent studies have also shown that IL-1β, TNF-α, or IFN-γ/

TNF-α–induced increases in intestinal TJ permeability were mediated in part by an increase in MLCK gene and protein expression and that the inhibition of MLCK expression or kinase activity prevented the increase in TJ permeability (23, 24, 60, 61). It has also been shown that MEKK1 and ERK1/2-dependent transcription factors NF-κB and Elk-1 are important regulators of MLCK gene activity (23, 62). However, the regulatory role of the p38 kinase pathway on MLCK gene regulation remains unclear. In this study, we show that the p38 kinase pathway plays an essential regulatory role in IL-1β modulation of MLCK gene activity. Our data indicated that IL-1β causes a rapid activation of p38 kinase in intestinal cells, and that inhibition of p38 kinase prevented the IL-1β–induced activation of MLCK gene and mRNA expression and the subsequent increase in Caco-2 TJ permeability. Our data indicated that the IL-1β–induced increases in MLCK gene activity and TJ permeability were dependent on p38 kinase activation.

Nuclear transcription factor ATF-2 is a member of the leucine zipper family of DNA-binding proteins and binds to the cAMP responsive element (63, 64). ATF-2 is a direct substrate of p38 kinase and is phosphorylated at Thr^{69}, Thr^{71}, and Ser^{91}, and Thr^{69} and Thr^{71} phosphorylation are necessary for ATF-2 activation and gene regulation (63, 64). ATF-2 has been shown to play an important role in many of the inflammatory responses regulated by the p38 kinase pathway, including cell proliferation, cytokine expression, and cell adhesion molecule expression (33, 65). However, the role of ATF-2 in intestinal TJ barrier regulation has not been previously reported. Our studies indicated that the IL-1β–induced p38 kinase activation leads to the phosphorylation and activation of ATF-2 in the intestinal cells. Additionally, using computer software, the ATF-2 binding motif was identified on the MLCK promoter region. Thus, we hypothesized that ATF-2 is a transcription factor that mediates p38 kinase activation of the MLCK gene and increases in TJ permeability. Our results indicated that the p38 kinase pathway induces the activation and nuclear translocation of ATF-2 in Caco-2 monolayers, and the promoter binding studies demonstrated the binding of activated ATF-2 to the cAMP-responsive element (AGCCACCCAT) on the MLCK promoter region (−268 to −259). Moreover, the siRNA-induced silencing of ATF-2 confirmed the requirement of ATF-2 for the increase in MLCK promoter activity and Caco-2 TJ permeability. The site-directed mutagenesis studies identified the specific molecular determinants responsible for the IL-1β regulation of the promoter activity and increase in Caco-2 TJ permeability. Taken together, these studies suggested that p38 kinase activation of ATF-2 leads to an activation of MLCK promoter activity and subsequent MLCK mRNA transcription and translation and MLCK-dependent opening of the Caco-2 TJ barrier.

In this study, we also investigated the in vivo relevance of p38 kinase and ATF-2 activation in the regulation of intestinal permeability in the mouse small intestine. Using a recently introduced in vivo gene silencing methodology, we were able to decipher the role of p38 kinase and ATF-2 in the in vivo regulation of MLCK gene expression and intestinal permeability (26). The in vivo studies indicated that IL-1β causes an activation of p38 kinase and ATF-2 in mouse small intestine. The p38 kinase–dependent activation of ATF-2 was required for the IL-1β–induced increase in intestinal MLCK expression and increase in mouse intestinal permeability. Thus, our studies confirmed that the p38 kinase pathway and ATF-2 were important regulators of MLCK activity and intestinal permeability in vivo.

Previous studies from our laboratory also suggested that IL-1β modulation of the Caco-2 TJ barrier was dependent in part on MAPK kinase MEKK-1 activation of NF-κB and MLCK gene activity (23, 24, 62). An intriguing question persists as to how the different signaling pathways and transcription factors cross-talk or interact to regulate the intestinal TJ barrier function. Our initial studies to decipher the cross-talk suggested that IL-1β–induced activation of MEKK-1 was not required for the p38 kinase activation or ATF-2 activation (data not shown). Interestingly, IL-1β–induced IκB-α degradation and NF-κB activation were dependent in part on p38 kinase activation, suggesting a cross-talk at the level of p38 kinase and inhibitory κB kinase. Our initial studies also suggested the possibility that ATF-2 may have a direct regulatory effect on NF-κB binding to the DNA binding site (data not shown). An important focus of our future research will be to decipher the precise cross-talk between the two signaling pathways and to identify the specific mechanisms and molecular interactions that mediate IL-1β modulation of intestinal TJ permeability.

In conclusion, our results provide new insight into the intracellular and molecular mechanisms that regulate the IL-1β modulation of intestinal TJ permeability. Our studies suggest that IL-1β–induced activation of p38 kinase causes a rapid phosphorylation and activation of ATF-2; the activated ATF-2 translocates to the nucleus and binds to the MLCK promoter, leading to MLCK gene activation, transcription, protein expression, and MLCK-dependent opening of the intestinal TJ barrier. Our data show the mechanism where the p38 kinase signaling cascade plays an essential role in mediating IL-1β modulation of the intestinal TJ barrier by targeting MLCK gene activity. These studies also show that transcription factor ATF-2 plays a key role in TJ barrier regulation by regulating MLCK promoter activity and gene expression. Additionally, our in vivo studies also demonstrate the feasibility of therapeutic targeting of p38 kinase and ATF-2 to prevent the cytokine-induced increase in intestinal TJ permeability in vivo.

Acknowledgments

We acknowledge the University of New Mexico Cancer Center Fluorescence Microsopy Shared Resource for providing clerical and technical assistance in generating images.

Disclosures

The authors have no financial conflicts of interest.

References

1. Arrieta, M. C., K. Madsen, J. Doyle, and J. Meddings. 2009. Reducing small intestinal permeability attenuates colitis in the IL10 gene-deficient mouse. *Gut* 58: 41–48.
2. Hollander, D. 1999. Intestinal permeability, leaky gut, and intestinal disorders. *Curr. Gastroenterol. Rep.* 1: 410–416.
3. Turner, J. R. 2009. Intestinal mucosal barrier function in health and disease. *Nat. Rev. Immunol.* 9: 799–809.
4. Ma, T. Y., and J. M. Anderson. 2012. Tight junctions and the intestinal barrier. In *Physiology of the Gastrointestinal Tract.* L. Johnson, ed. Elsevier Academic Press, Burlington, MA, p. 1043–1088.
5. Hollander, D. 1988. Crohn's disease: a permeability disorder of the tight junction? *Gut* 29: 1621–1624.
6. Arnott, I. D., D. Watts, and S. Ghosh. 2002. Review article: is clinical remission the optimum therapeutic goal in the treatment of Crohn's disease? *Aliment. Pharmacol. Ther.* 16: 857–867.
7. Madsen, K. L. 2001. Inflammatory bowel disease: lessons from the IL-10 gene-deficient mouse. *Clin. Invest. Med.* 24: 250–257.
8. Madsen, K. L., D. Malfair, D. Gray, J. S. Doyle, L. D. Jewell, and R. N. Fedorak. 1999. Interleukin-10 gene-deficient mice develop a primary intestinal permeability defect in response to enteric microflora. *Inflamm. Bowel Dis.* 5: 262–270.
9. Cominelli, F., C. C. Nast, B. D. Clark, R. Schindler, R. Lierena, V. E. Eysselein, R. C. Thompson, and C. A. Dinarello. 1990. Interleukin 1 (IL-1) gene expression, synthesis, and effect of specific IL-1 receptor blockade in rabbit immune complex colitis. *J. Clin. Invest.* 86: 972–980.
10. Dinarello, C. A. 1994. Interleukin-1 in disease. *Keio J. Med.* 43: 131–136.
11. Al-Sadi, R. M., and T. Y. Ma. 2007. IL-1β causes an increase in intestinal epithelial tight junction permeability. *J. Immunol.* 178: 4641–4649.

12. Cominelli, F., and T. T. Pizarro. 1996. Interleukin-1 and interleukin-1 receptor antagonist in inflammatory bowel disease. *Aliment. Pharmacol. Ther.* 10(Suppl 2): 49–53, discussion 54.
13. Dinarello, C. A. 1996. Biologic basis for interleukin-1 in disease. *Blood* 87: 2095–2147.
14. O'Neill, L. A., and C. A. Dinarello. 2000. The IL-1 receptor/Toll-like receptor superfamily: crucial receptors for inflammation and host defense. *Immunol. Today* 21: 206–209.
15. Nemetz, A., M. P. Nosti-Escanilla, T. Molnár, A. Köpe, A. Kovács, J. Fehér, Z. Tulassay, F. Nagy, M. A. García-González, and A. S. Peña. 1999. *IL1B* gene polymorphisms influence the course and severity of inflammatory bowel disease. *Immunogenetics* 49: 527–531.
16. Carvalho, F. A., J. D. Aitken, A. T. Gewirtz, and M. Vijay-Kumar. 2011. TLR5 activation induces secretory interleukin-1 receptor antagonist (sIL-1Ra) and reduces inflammasome-associated tissue damage. *Mucosal Immunol.* 4: 102–111.
17. Hultgren, O. H., M. Berglund, M. Bjursten, and E. Hultgren Hörnquist. 2006. Serum interleukin-1 receptor antagonist is an early indicator of colitis onset in Gαi2-deficient mice. *World J. Gastroenterol.* 12: 621–624.
18. Carter, J. D., J. Valeriano, and F. B. Vasey. 2003. Crohn disease worsened by anakinra administration. *J. Clin. Rheumatol.* 9: 276–277.
19. Alten, R., H. Gram, L. A. Joosten, W. B. van den Berg, J. Sieper, S. Wassenberg, G. Burmester, P. van Riel, M. Diaz-Lorente, G. J. Bruin, et al. 2008. The human anti-IL-1β monoclonal antibody ACZ885 is effective in joint inflammation models in mice and in a proof-of-concept study in patients with rheumatoid arthritis. *Arthritis Res. Ther.* 10: R67.
20. Brun, P., I. Castagliuolo, V. Di Leo, A. Buda, M. Pinzani, G. Palù, and D. Martines. 2007. Increased intestinal permeability in obese mice: new evidence in the pathogenesis of nonalcoholic steatohepatitis. *Am. J. Physiol. Gastrointest. Liver Physiol.* 292: G518–G525.
21. Jin, W., H. Wang, Y. Ji, Q. Hu, W. Yan, G. Chen, and H. Yin. 2008. Increased intestinal inflammatory response and gut barrier dysfunction in Nrf2-deficient mice after traumatic brain injury. *Cytokine* 44: 135–140.
22. Al-Sadi, R., M. Boivin, and T. Ma. 2009. Mechanism of cytokine modulation of epithelial tight junction barrier. *Front. Biosci.* 14: 2765–2778.
23. Al-Sadi, R., D. Ye, K. Dokladny, and T. Y. Ma. 2008. Mechanism of IL-1β-induced increase in intestinal epithelial tight junction permeability. *J. Immunol.* 180: 5653–5661.
24. Al-Sadi, R., D. Ye, H. M. Said, and T. Y. Ma. 2011. Cellular and molecular mechanism of interleukin-1β modulation of Caco-2 intestinal epithelial tight junction barrier. *J. Cell. Mol. Med.* 15: 970–982.
25. Lu, D. Q., J. X. Bei, L. N. Feng, Y. Zhang, X. C. Liu, L. Wang, J. L. Chen, and H. R. Lin. 2008. Interleukin-1β gene in orange-spotted grouper, *Epinephelus coioides*: molecular cloning, expression, biological activities and signal transduction. *Mol. Immunol.* 45: 857–867.
26. Armstrong, M. E., C. E. Loscher, M. A. Lynch, and K. H. Mills. 2003. IL-1β-dependent neurological effects of the whole cell pertussis vaccine: a role for IL-1-associated signalling components in vaccine reactogenicity. *J. Neuroimmunol.* 136: 25–33.
27. Boivin, M. A., D. Ye, J. C. Kennedy, R. Al-Sadi, C. Shepela, and T. Y. Ma. 2007. Mechanism of glucocorticoid regulation of the intestinal tight junction barrier. *Am. J. Physiol. Gastrointest. Liver Physiol.* 292: G590–G598.
28. Clayburgh, D. R., T. A. Barrett, Y. Tang, J. B. Meddings, L. J. Van Eldik, D. M. Watterson, L. L. Clarke, R. J. Mrsny, and J. R. Turner. 2005. Epithelial myosin light chain kinase-dependent barrier dysfunction mediates T cell activation-induced diarrhea in vivo. *J. Clin. Invest.* 115: 2702–2715.
29. Al-Sadi, R., K. Khatib, S. Guo, D. Ye, M. Youssef, and T. Ma. 2011. Occludin regulates macromolecule flux across the intestinal epithelial tight junction barrier. *Am. J. Physiol. Gastrointest. Liver Physiol.* 300: G1054–G1064.
30. Clayburgh, D. R., S. Rosen, E. D. Witkowski, F. Wang, S. Blair, S. Dudek, J. G. Garcia, J. C. Alverdy, and J. R. Turner. 2004. A differentiation-dependent splice variant of myosin light chain kinase, MLCK1, regulates epithelial tight junction permeability. *J. Biol. Chem.* 279: 55506–55513.
31. Ye, D., S. Guo, R. Al-Sadi, and T. Y. Ma. 2011. MicroRNA regulation of intestinal epithelial tight junction permeability. *Gastroenterology* 141: 1323–1333.
32. Ma, T. Y., G. K. Iwamoto, N. T. Hoa, V. Akotia, A. Pedram, M. A. Boivin, and H. M. Said. 2004. TNF-α-induced increase in intestinal epithelial tight junction permeability requires NF-κB activation. *Am. J. Physiol. Gastrointest. Liver Physiol.* 286: G367–G376.
33. Kumar, S., P. C. McDonnell, R. J. Gum, A. T. Hand, J. C. Lee, and P. R. Young. 1997. Novel homologues of CSBP/p38 MAP kinase: activation, substrate specificity and sensitivity to inhibition by pyridinyl imidazoles. *Biochem. Biophys. Res. Commun.* 235: 533–538.
34. Arana-Argáez, V. E., V. Delgado-Rizo, O. E. Pizano-Martínez, E. A. Martínez-Garcia, B. T. Martín-Márquez, A. Muñoz-Gómez, M. H. Petri, J. Armendáriz-Borunda, G. Espinosa-Ramírez, D. A. Zúñiga-Tamayo, et al. 2010. Inhibitors of MAPK pathway ERK1/2 or p38 prevent the IL-1β-induced up-regulation of SRP72 autoantigen in Jurkat cells. *J. Biol. Chem.* 285: 32824–32833.
35. Kim, Y. J., S. Y. Hwang, E. S. Oh, S. Oh, and I. O. Han. 2006. IL-1β, an immediate early protein secreted by activated microglia, induces iNOS/NO in C6 astrocytoma cells through p38 MAPK and NF-κB pathways. *J. Neurosci. Res.* 84: 1037–1046.
36. Ahmad, R., J. Sylvester, and M. Zafarullah. 2007. MyD88, IRAK1 and TRAF6 knockdown in human chondrocytes inhibits interleukin-1-induced matrix metalloproteinase-13 gene expression and promoter activity by impairing MAP kinase activation. *Cell. Signal.* 19: 2549–2557.
37. Rossa, C., K. Ehmann, M. Liu, C. Patil, and K. L. Kirkwood. 2006. MKK3/6-p38 MAPK signaling is required for IL-1β and TNF-α-induced RANKL expression in bone marrow stromal cells. *J. Interferon Cytokine Res.* 26: 719–729.
38. Gan, H. T., and J. D. Chen. 2007. Induction of heme oxygenase-1 improves impaired intestinal transit after burn injury. *Surgery* 141: 385–393.
39. Saldeen, J., J. C. Lee, and N. Welsh. 2001. Role of p38 mitogen-activated protein kinase (p38 MAPK) in cytokine-induced rat islet cell apoptosis. *Biochem. Pharmacol.* 61: 1561–1569.
40. Yang, C. M., H. L. Hsieh, and C. W. Lee. 2005. Intracellular signaling mechanisms underlying the expression of pro-inflammatory mediators in airway diseases. *Chang Gung Med. J.* 28: 813–823.
41. Holden, N. S., M. C. Catley, L. M. Cambridge, P. J. Barnes, and R. Newton. 2004. ICAM-1 expression is highly NF-κB-dependent in A549 cells. No role for ERK and p38 MAPK. *Eur. J. Biochem.* 271: 785–791.
42. Kacimi, R., J. S. Karliner, F. Koudssi, and C. S. Long. 1998. Expression and regulation of adhesion molecules in cardiac cells by cytokines: response to acute hypoxia. *Circ. Res.* 82: 576–586.
43. Krishnaveni, M., and S. Jayachandran. 2009. Inhibition of MAP kinases and down regulation of TNF-α, IL-β and COX-2 genes by the crude extracts from marine bacteria. *Biomed. Pharmacother.* 63: 469–476.
44. Liang, K. C., C. W. Lee, W. N. Lin, C. C. Lin, C. B. Wu, S. F. Luo, and C. M. Yang. 2007. Interleukin-1β induces MMP-9 expression via p42/p44 MAPK, p38 MAPK, JNK, and nuclear factor-κB signaling pathways in human tracheal smooth muscle cells. *J. Cell. Physiol.* 211: 759–770.
45. Masamune, A., M. Satoh, K. Kikuta, Y. Sakai, A. Satoh, and T. Shimosegawa. 2003. Inhibition of p38 mitogen-activated protein kinase blocks activation of rat pancreatic stellate cells. *J. Pharmacol. Exp. Ther.* 304: 8–14.
46. Jackson, J. R., B. Bolognese, L. Hillegass, S. Kassis, J. Adams, D. E. Griswold, and J. D. Winkler. 1998. Pharmacological effects of SB 220025, a selective inhibitor of p38 mitogen-activated protein kinase, in angiogenesis and chronic inflammatory disease models. *J. Pharmacol. Exp. Ther.* 284: 687–692.
47. Docena, G., L. Rovedatti, L. Kruidenier, A. Fanning, N. A. Leakey, C. H. Knowles, K. Lee, F. Shanahan, K. Nally, P. G. McLean, et al. 2010. Down-regulation of p38 mitogen-activated protein kinase activation and proinflammatory cytokine production by mitogen-activated protein kinase inhibitors in inflammatory bowel disease. *Clin. Exp. Immunol.* 162: 108–115.
48. Waetzig, G. H., D. Seegert, P. Rosenstiel, S. Nikolaus, and S. Schreiber. 2002. p38 Mitogen-activated protein kinase is activated and linked to TNF-α signaling in inflammatory bowel disease. *J. Immunol.* 168: 5342–5351.
49. Wang, Q., X. L. Guo, D. Wells-Byrum, G. Noel, T. A. Pritts, and C. K. Ogle. 2008. Cytokine-induced epithelial permeability changes are regulated by the activation of the p38 mitogen-activated protein kinase pathway in cultured Caco-2 cells. *Shock* 29: 531–537.
50. Costantini, T. W., C. Y. Peterson, L. Kroll, W. H. Loomis, B. P. Eliceiri, A. Baird, V. Bansal, and R. Coimbra. 2009. Role of p38 MAPK in burn-induced intestinal barrier breakdown. *J. Surg. Res.* 156: 64–69.
51. Oshima, T., H. Miwa, and T. Joh. 2008. Aspirin induces gastric epithelial barrier dysfunction by activating p38 MAPK via claudin-7. *Am. J. Physiol. Cell Physiol.* 295: C800–C806.
52. Patrick, D. M., A. K. Leone, J. J. Shellenberger, K. A. Dudowicz, and J. M. King. 2006. Proinflammatory cytokines tumor necrosis factor-α and interferon-γ modulate epithelial barrier function in Madin-Darby canine kidney cells through mitogen activated protein kinase signaling. *BMC Physiol.* 6: 2.
53. Kevil, C. G., T. Oshima, and J. S. Alexander. 2001. The role of p38 MAP kinase in hydrogen peroxide mediated endothelial solute permeability. *Endothelium* 8: 107–116.
54. Campbell, M., R. Collery, A. McEvoy, T. A. Gardiner, A. W. Stitt, and B. Brankin. 2006. Involvement of MAPKs in endostatin-mediated regulation of blood-retinal barrier function. *Curr. Eye Res.* 31: 1033–1045.
55. Hecht, G., and A. Koutsouris. 1999. Myosin regulation of NKCC1: effects on cAMP-mediated Cl^- secretion in intestinal epithelia. *Am. J. Physiol.* 277: C441–C447.
56. Ma, T. Y., N. T. Hoa, D. D. Tran, V. Bui, A. Pedram, S. Mills, and M. Merryfield. 2000. Cytochalasin B modulation of Caco-2 tight junction barrier: role of myosin light chain kinase. *Am. J. Physiol. Gastrointest. Liver Physiol.* 279: G875–G885.
57. Ma, T. Y., D. Nguyen, V. Bui, H. Nguyen, and N. Hoa. 1999. Ethanol modulation of intestinal epithelial tight junction barrier. *Am. J. Physiol.* 276: G965–G974.
58. Ma, T. Y., D. Tran, N. Hoa, D. Nguyen, M. Merryfield, and A. Tarnawski. 2000. Mechanism of extracellular calcium regulation of intestinal epithelial tight junction permeability: role of cytoskeletal involvement. *Microsc. Res. Tech.* 51: 156–168.
59. Madara, J. L., R. Moore, and S. Carlson. 1987. Alteration of intestinal tight junction structure and permeability by cytoskeletal contraction. *Am. J. Physiol.* 253: C854–C861.
60. Turner, J. R., B. K. Rill, S. L. Carlson, D. Carnes, R. Kerner, R. J. Mrsny, and J. L. Madara. 1997. Physiological regulation of epithelial tight junctions is associated with myosin light-chain phosphorylation. *Am. J. Physiol.* 273: C1378–C1385.
61. Ye, D., I. Ma, and T. Y. Ma. 2006. Molecular mechanism of tumor necrosis factor-α modulation of intestinal epithelial tight junction barrier. *Am. J. Physiol. Gastrointest. Liver Physiol.* 290: G496–G504.
62. Al-Sadi, R., D. Ye, H. M. Said, and T. Y. Ma. 2010. IL-1β-induced increase in intestinal epithelial tight junction permeability is mediated by MEKK-1 activation of canonical NF-κB pathway. *Am. J. Pathol.* 177: 2310–2322.
63. Gupta, S., D. Campbell, B. Dérijard, and R. J. Davis. 1995. Transcription factor ATF2 regulation by the JNK signal transduction pathway. *Science* 267: 389–393.
64. Livingstone, C., G. Patel, and N. Jones. 1995. ATF-2 contains a phosphorylation-dependent transcriptional activation domain. *EMBO J.* 14: 1785–1797.
65. Ricote, M., I. García-Tuñón, F. Bethencourt, B. Fraile, P. Onsurbe, R. Paniagua, and M. Royuela. 2006. The p38 transduction pathway in prostatic neoplasia. *J. Pathol.* 208: 401–407.